ELSEVIER

Journal of Alloys and Compounds 425 (2006) 129–139

Journal of ALLOYS AND COMPOUNDS

www.elsevier.com/locate/jallcom

A computational thermodynamic model of the Mg–Al–Ge system

F. Islam, A.K. Thykadavil, M. Medraj *

Department of Mechanical and Industrial Engineering, Concordia University, 1455 de Maisonneuve West, Montreal, Que., Canada H3G 1M8

Received 27 October 2005; received in revised form 2 December 2005; accepted 4 January 2006
Available online 9 May 2006

Abstract

The Mg–Al–Ge system has been thermodynamically modeled by combining thermodynamic description of the three constituent binary systems and using a ternary interaction parameter for the liquid phase. Among the three binary systems, Mg–Ge and Al–Ge systems are optimized in this study, whereas the optimized thermodynamic parameters for the Al–Mg system are taken from COST 507 database. The binary excess energy terms are described using Redlich–Kister polynomial model. The ternary invariant points are predicted from the thermodynamic model. The Mg–Al–Ge phase diagram has been modeled for the first time in this work and found to be consistent with the experimental results available in the literature.
© 2006 Elsevier B.V. All rights reserved.

Keywords: Thermodynamic modeling; Mg–Al based alloys; Al–Ge system; Mg–Ge system; Mg–Al–Ge system

1. Introduction

Magnesium is the lightest structural material with a density of 1.741 g/cm^3. This makes Mg alloys particularly attractive for transportation applications. New Mg alloys with lower cost and superior properties are desirable, if wider applications of Mg alloys are to be developed [1]. Although Mg–Al–Ge system has not yet been studied that much, several studies have been carried out for the similar Mg–Al–Si system, which is widely used in aerospace and automotive industries. These studies show a great potential for Mg–Al–Ge system because it is difficult to determine the atomic position of the precipitate in a unit cell due to the similarity of atomic weight and scattering factor of Si and Mg. Hence, replacing Si by Ge can resolve this issue since Ge and Si are homologous but with higher atomic weight for Ge [2]. Moreover, aluminum mechanically alloyed with Mg and Ge exhibits improved super plastic elongation [3]. Properties of these alloys are to a great extent determined by the formation of intermetallic compounds. It is necessary to know the phase diagram and thermodynamic description of Mg–Al–Ge system to develop alloys with required properties in this system. In order to develop the thermodynamic description of this ternary system, the thermodynamic properties of the constituent binaries must be known. Hence, the Mg–Ge and Al–Ge systems have been optimized in this study using both the experimental phase diagram and the thermodynamic data available in the literature. The third system, Al–Mg, has been taken from COST 507 [4] database, as this database is the most recent and reliable. The liquid phase for the ternary system has also been modeled. For binary and ternary systems, the calculated results from this study are compared with the experimental results available in the literature.

Phase diagrams are extremely important for the development of new alloys and processing of materials. Experiments on a technological scale for preparation and testing of new alloys are very expensive and time consuming. Computational thermochemistry, based on the Calculation of Phase Diagram (CALPHAD) approach, is a powerful tool that supplies quantitative data to guide the development of alloys or the optimization of materials processing in a cost effective way [5]. Phase relations in a ternary system are of primary importance; they involve thermodynamic properties of the system and can be fully understood through computational thermodynamics. In order to describe the thermodynamic properties of a ternary system, the thermodynamic properties of the associated binary systems should be known.

A system is at equilibrium when its free energy is at a minimum. For the calculation of phase equilibrium in a multicomponent system, it is necessary to minimize the total Gibbs energy of all the phases that take part in this equilibrium as:

$$G = \sum_{\varphi=1}^{p} n^{\varphi} G^{\varphi} \tag{1}$$

* Corresponding author. Tel.: +1 514 848 2424x3146; fax: +1 514 848 3175.
E-mail address: mmedraj@encs.concordia.ca (M. Medraj).

0925-8388/$ – see front matter © 2006 Elsevier B.V. All rights reserved.
doi:10.1016/j.jallcom.2006.01.050

In Eq. (1), G represents the total Gibbs energy of all the phases, n_φ the number of moles of phase φ, p the number of phases and G_φ is the Gibbs energy of phase φ [5].

A thermodynamic description of a system requires the knowledge of thermodynamic functions of each phase. The Gibbs energy of the pure element i with a certain structure phase φ, referred to the enthalpy of its standard state, at 298.15 K is described in terms of temperature by Eq. (2) [6]:

$$^0G_i^\varphi(T) = a + bT + cT\ \ln(T) + dT^2 + eT^3 + fT^{-1} + gT^7 + hT^{-9} \quad (2)$$

where a, b, …, h are coefficients and the values are assigned from SGTE database [6].

The solution phases such as liquid and disordered solid solution phases, the composition and temperature dependence of the Gibbs energy are described using a regular-solution type model as:

$$G_{\text{Liq}}^{\text{ø}} = \sum_{i=1}^{n} x_i^0 G_i^\varphi + RT\sum_{i=1}^{n} x_i\ \ln(x_i) + G^{\text{ex},\varphi} \quad (3)$$

In Eq. (3), x_i is the mole fraction of the component i, $^0G_i^\varphi$ the Gibbs energy of pure component i with structure φ, R is the gas constant and T is temperature. The first term in Eq. (3) corresponds to the mechanical mixture of the pure elements constituting the phase, the second term corresponds to Gibbs energy of mixing for an ideal solution and the third term represents the Gibbs excess energy. The Gibbs excess energy is represented as:

$$G^{\text{ex},\varphi} = \sum_{i,j=1(i\neq j)}^{n} x_i x_j \sum_{k=0}^{m} L_{(i,j)}^k (x_i - x_j)^K + \sum_{i,j,l=1(i\neq j\neq l)}^{n} x_i x_j x_l \sum_{k=i,j,l} L^k V^k \quad (4)$$

In Eq. (4) the first term is the binary interaction term for i–j binary and second term is ternary interactions for i–j–l system, where $L_{(i,j)}^k$ and L^k are the binary and ternary interaction parameters, respectively, and can be represented by $L^k = a_k + b_k T$, where a_k and b_k are determined from experimental data (e.g., phase diagram and thermodynamic data) using least-squares method. The determination of coefficients from experimental data in this manner is known as thermodynamic optimization [7]. V_k is defined as:

$$V_k = x_k + \frac{1 - \sum_{q=i,j,l} x_q}{n} \quad (5)$$

The Gibbs energy of a binary stoichiometric phase is given by Eq. (6).

$$G_{\text{stoichiometric}}^\varphi = \sum_{i=1}^{n} x_i^0 G_i^\varphi + \Delta G_{\text{f}} \quad (6)$$

where $\Delta G_{\text{f}} = a + bT$ represents the Gibbs energy of formation per mole of atom of the stoichiometric compound and a and b are obtained by optimization of the phase equilibria and thermodynamic data.

The thermodynamic descriptions of subsystems, which are part of a higher order system, must be same if the higher order system is to be combined [8]. During calculation of ternary phase diagram, the model descriptions of the phases present in the three binary systems must be consistent so that the descriptions of the same phase occurring in more than one binary system can be combined. Thermodynamic extrapolation methods are used to extend the thermodynamic functions of the binary into ternary and higher order systems. Using the results of the extrapolations, critical experiments can be designed and thereby experimental work can be minimized. Using optimized binary subsystems, the phase diagram of ternary or quaternary systems can be developed with reasonable accuracy [9]. For this work, the computer program WinPhaD [10] is used for optimizing the binary subsystems Mg–Ge and Al–Ge.

2. The Al–Ge system

2.1. Equilibrium diagram

The Al–Ge eutectic system consists of three phases: (i) the liquid; (ii) the Al-fcc solid solution with cF4-type structure; (iii) Ge-diamond cubic solid solution with cF8-type structure. There is one invariant equilibrium point in this system. High-pressure metastable phases of Al–Ge alloys are superconducting in nature, and these alloys when amorphised are good semiconductors [11]. Most of the experimental data available are that of the liquidus, only a few researchers have studied solvus and solidus portions.

The Al–Ge liquidus was studied using thermal analysis by Kroll [12] and Stohr and Klemm [13]. Wilder [14] and Eslami et al. [15] studied the Ge-rich portion of the Al–Ge liquidus, using electrochemical method. Stohr and Klemm [13] studied the Al-rich solvus below the eutectic temperature using X-ray diffraction of heat treated and quenched samples. Using heat treated Al films on Ge substrates, Caywood [16] performed He+ backscattering experiments for studying the Al-rich solvus. Glazov et al. [17] studied the Ge-rich solidus above the eutectic temperature using optical microscopy and microhardness testing on heat treated and quenched samples. The most recent study is by Minamino et al. [18] who determined the solidus and solubility limits in the Al-fcc using electron probe microanalysis.

2.2. Thermodynamics

Wilder [14] determined the activity of Al in Al–Ge system using reversible galvanic cell. The value of partial Gibbs free energy of mixing, partial entropy of mixing and partial enthalpy of mixing of Al were determined from the activity values. Using Gibbs–Duhem equation, the thermodynamic properties of Ge were determined from the corresponding values of Al. Batalin and Belaborodova [19] determined the activities of Al in the Al–Ge system at 1273 K using electrochemical measurements. They also measured the integral enthalpy of mixing of Al–Ge system. Using calorimetric measurements, Predel and Stein [20] determined the integral enthalpy of mixing of Al–Ge liquid at 1273 K. In their work, other thermodynamic properties such as

activities, partial enthalpy of mixing of Al and Ge, integral and partial entropy of mixing and integral and partial Gibbs free energies of Al and Ge at 1273 K were also calculated. However, Eslami et al. [21] determined the integral enthalpy of mixing of Al–Ge liquid at 1235 K using direct reaction calorimetry. The thermodynamic properties determined by various researchers are in good agreement with each other.

2.3. Optimization of thermodynamic properties and phase diagram

McAlister and Murray [22] optimized the Al–Ge system using experimental phase diagram data and thermodynamic properties from various researchers. During their optimization, experimental data for Ge-rich solvus and solidus at Al end were not available and hence they were not included. They performed the optimization using non-linear least-squares technique, and placed the Al–Ge eutectic at 28.4 at.% Ge, and 693 K. Srikanth et al. [11] reoptimized the Al–Ge system by including the Al-rich solvus and solidus data of Minamino et al. [18] and arrived at the eutectic point of 28 at.% Ge at 696.85 K. Since the thermodynamic parameters of hypothetical diamond cubic Al are not given in the SGTE database [6], they derived them by combining the SGTE data [6] for liquid Al with the recommended data of Kaufman [23] given with reference to pure liquid Al. They also calculated thermodynamic properties such as enthalpy of mixing of liquid Al–Ge alloys, partial enthalpy of mixing of Al and partial entropy of mixing of Al. Their calculated thermodynamic properties were in good agreement with experimental data from the literature. Though Srikanth et al. [11] and McAlister and Murray [22] reported the optimized parameters but the total number of parameters was high and they also used additional lattice stability values for pure elements. As physically sound models are more informative and need less adjustable parameters to fit the experimental data [8], this system is reoptimized with the purpose of finding less number of parameters.

In the current work, the Al-rich solvus and solidus data determined by Minamino et al. [18], liquidus data of Wilder [14] and integral enthalpy of mixing of liquid Al–Ge alloy of Predel and Stein [20], Eslami et al. [21] and Batalin and Belaborodova [19] and activity values of Al reported by Wilder [14] and Batalin and Belaborodova [19] are used for optimization. Thermodynamic parameters of hypothetical diamond cubic Al derived by Srikanth et al. [11] are used. Lattice stability values are not added for pure elements to keep consistency with other binary systems in this study. The phase diagram and predicted thermodynamic properties such as partial enthalpy of mixing and partial Gibbs energy of Al are calculated from the optimized model parameters.

Table 1
Optimized model parameters for Al–Ge and Mg–Ge systems

System	Phase	Parameter	a (J/(mol atom))	b (J/(mol atom K))
Al–Ge	Liquid	L_0	−14869	−1.10
		L_1	3325	−3.67
Al–Ge	fcc	L_0	20563.52	−28.76
Al–Ge	Diamond	L_0	16980.04	−22.49
Mg–Ge	Liquid	L_0	−98280.75	19.24
		L_1	−72100	44.57
		L_2	4097.10	7.53
		L_3	50595.53	−27.95
Mg–Ge	Mg_2Ge	ΔG_f	−39372.77	7.98
Mg–Al–Ge	Liquid	L_0	−55486.30	20.00

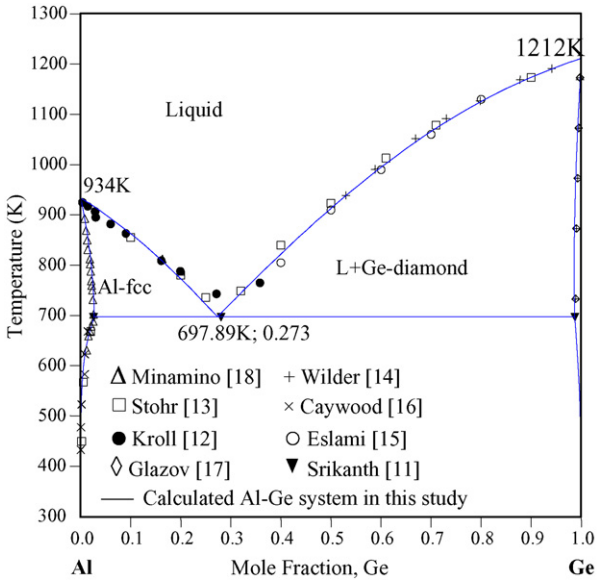

Fig. 1. Calculated Al–Ge phase diagram with experimental points.

A two terms Redlich–Kister polynomial equation for the liquid and single term Redlich–Kister equation for the Ge and Al solid solutions are used for this optimization. The optimized binary parameters for the Al–Ge system are given in Table 1. The calculated binary invariant point is presented in Table 2.

Fig. 1 shows the calculated Al–Ge phase diagram with experimental data from various researchers.

Figs. 2–5 show the calculated thermodynamic properties of liquid Al–Ge system in relation to experimental data from the literature.

Table 2
Comparison of phase equilibrium results of the Al–Ge and Mg–Ge systems

System	Reaction	Current work (at.% Ge), T (K)	Literature value (at.% Ge), T (K)	Reference
Al–Ge	Liquid → Al-fcc + Ge-diamond	27.33, 697.89	28, 696.9	[11]
Mg–Ge	Liquid → Mg_2Ge + Ge-diamond	65.1, 969.4	64.3, 969.9	[24]
	Liquid → Mg-hcp + Mg_2Ge	2.6, 904	1.2, 908.8	[25]
	Liquid → Mg_2Ge	33.33, 1390.5	1390.6	[24]

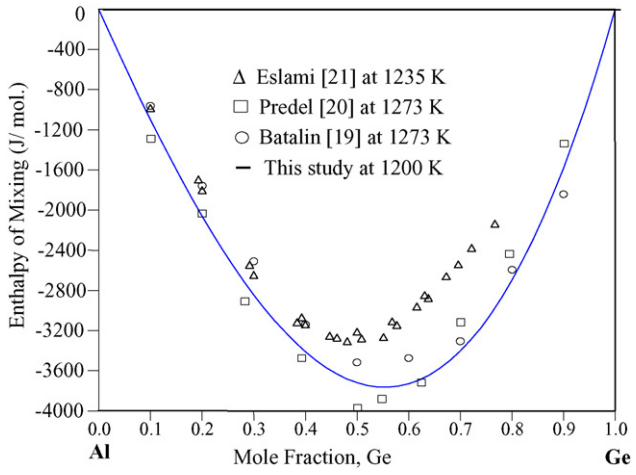

Fig. 2. Enthalpy of mixing of Al–Ge liquid.

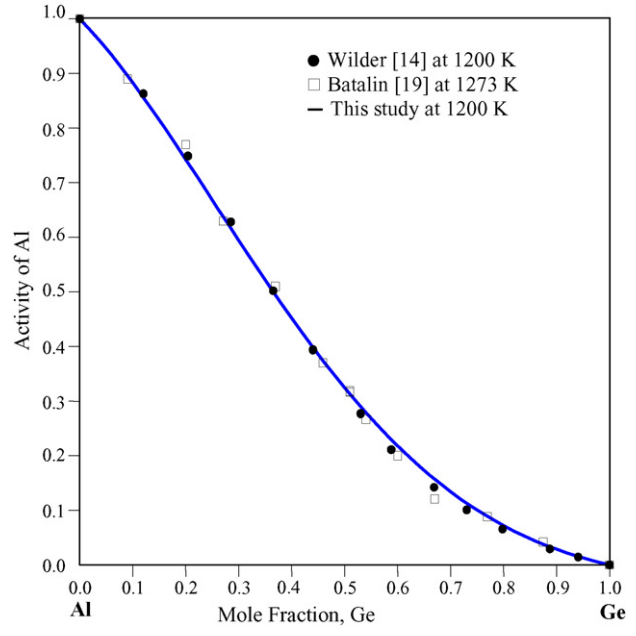

Fig. 3. Activity of Al in Al–Ge liquid.

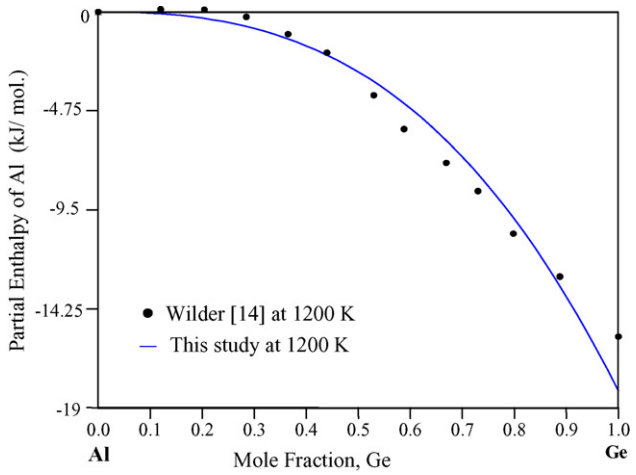

Fig. 4. Partial enthalpy of Al in Al–Ge liquid.

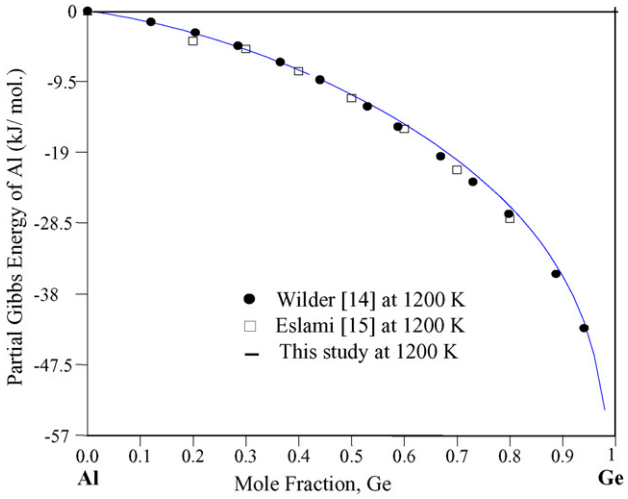

Fig. 5. Partial Gibbs energy of Al in Al–Ge liquid.

From the figures, it can be found that the calculated phase diagram and thermodynamic properties are in good agreement with experimental data reported in the literature. The predicted thermodynamic properties, such as partial enthalpy and partial Gibbs energy of Al presented, respectively, in Figs. 4 and 5 also show good agreement, which proves the quality of the model. During calculation of the thermodynamic properties the reference state of the pure elements Al and Ge is the liquid phase and the temperature is 1200 K.

3. The Mg–Ge system

3.1. Equilibrium diagram

The Mg–Ge system consists of: (i) the liquid; (ii) Mg-hcp terminal solid solution, with hp2-type structure with negligible solid solubility of Ge in Mg; (iii) Ge-diamond cubic terminal solid solution, with cf8-type structure with very low solubility of Mg in Ge; (iv) the Mg_2Ge compound, a semiconductor of stoichiometric composition with antifluoride cf12-type structure [26]. There are three invariant equilibria in this system: the eutectic on the Mg-rich side, the eutectic on the Ge-rich side and the congruent melting point of Mg_2Ge.

Klemm and Westlinning [27] first determined the Mg–Ge equilibrium phase diagram using thermal and microscopic analyses. But the purity of the starting materials was not mentioned and homogeneity was not maintained during cooling. Moreover, in the composition range of 33–50 at.% Ge, there was excessive Mg evaporation. Due to the inaccuracies in the liquidus data published by them, Geffken and Miller [24] reinvestigated the Mg–Ge system using thermal analysis and constructed the phase diagram. They [24] found Mg-rich eutectic temperature to be 908.75 K and it was in good agreement with the value of 908.15 K reported by Raynor [25]. Raynor [25] determined the composition of the Mg-rich eutectic as 1.15 at.% Ge. Using extrapolation, Geffken and Miller [24] determined the Ge-rich eutectic as 64.3 at.% Ge, against 61 at.% Ge reported by Klemm and Westlinning [27]. According to Geffken and Miller [24], the

temperature at the Ge-rich eutectic was 969.85 K, while Klemm and Westlinning [27] value was 953.15 K. However, Rao and Belton [28] constructed the liquidus of this phase diagram using emf method with a galvanic cell that had $MgCl_2$ as the electrolyte. The constructed phase diagram was found to be in good agreement with that of Klemm and Westlinning [27], but showed a difference of about 40–60 °C for most of the liquidus temperatures with that of Geffken and Miller [24]. Rao and Belton [28] disagree with the liquidus temperatures reported by Geffken and Miller [24] without explaining the source of error. Moreover, the sharp peak shown in the reported phase diagram of Rao and Belton [28] violates the Gibbs–Konovalov rule [26].

3.2. Thermodynamics

Eldridge et al. [29] determined the thermodynamic properties of liquid Mg–Ge alloys using isopiestic method between the temperature of 1000 and 1500 K. They calculated integral properties such as enthalpy, Gibbs energy and entropy of mixing and partial molar enthalpy and activity of Mg in the Mg–Ge liquid at 1388 K. Eldridge et al. [29] calculated the activity and partial molar enthalpy of Ge using Gibbs–Duhem equation and the corresponding values of Mg. They also determined that among the Mg–Group IVB systems, namely Mg–Pb, Mg–Sn, Mg–Ge and Mg–Si, the intermetallic compound Mg_2Ge had the maximum degree of ionicity and concluded that the bonding in Mg_2–Group IVB compounds was largely covalent. The heat of formation of $Mg_{0.67}Ge_{0.33}$ reported by Beardmore et al. [30] was in good agreement with the value determined by Eldridge et al. [29]. On the other hand, Geffken and Miller [24] calculated the activity values for Mg–Ge system using their phase diagram data, heat of formation of Mg_2Ge reported by Beardmore et al. [30] and partial molar enthalpy values obtained by Eldridge et al. [29]. They [24] found that there was very good agreement between the calculated activity values and those experimentally obtained by Eldridge et al. [29]. Hence, it was concluded that there was good consistency between the phase diagram of Geffken and Miller [24] and thermodynamic properties reported by Beardmore et al. [30] and Eldridge et al. [29].

Using emf method with $MgCl_2$ as the electrolyte, Rao and Belton [28] determined the thermodynamic properties of liquid Mg–Ge system. They found that the heat of formation of Mg_2Ge at 298 K from the solid elements is -104.23 ± 1.26 kJ, whereas Beardmore et al. [30] reported the same as -115.37 ± 0.25 kJ, showing a disagreement between the two values. Nevertheless, their results for the activities in the Ge-rich region were in very close agreement with those of Eldridge et al. [29]. But for the Mg-rich alloys, the results of Rao and Belton [28] were 12% lower than those reported by Eldridge et al. [29]. Rao and Belton pointed out that this discrepancy might be due to extrapolation to a common temperature in isopiestic measurements by Eldridge et al. [29]. The striking difference in the Rao and Belton [28] work was that they showed a most negative value for the partial molar enthalpy of Mg at infinite dilution, whereas Eldridge et al. [29] showed a minimum at around 18 at.% Mg.

By least-squares optimization of thermodynamic and liquidus data from various literature, Nayeb-Hashemi et al. [26] developed a polynomial expression for Gibbs excess free energy value for liquid Mg–Ge alloys. Using the polynomial expression and standard free energy of fusion of Mg, Ge and $Mg_{0.67}Ge_{0.33}$, they calculated the phase diagram. However, they did not present the various thermodynamic properties of the Mg–Ge liquid. Hence, the Mg–Ge binary system was reoptimized in this work.

The heat of formation of solid $Mg_{0.67}Ge_{0.33}$ ($(2/3)Mg_{(s)} + (1/3)Ge_{(s)} \rightarrow Mg_{0.67}Ge_{0.33(s)}$) has been determined by different researchers using emf, vapor pressure, tin solution calorimetry and direct reaction calorimetry methods and found to vary from -34.33 to -38.93 kJ/mol [26].

3.3. Optimization of thermodynamic properties and phase diagram

Similar to the Al–Ge system, the Mg–Ge system optimization is carried out by simultaneously optimizing the experimental thermodynamic and phase diagram data. The experimental phase diagram of Geffken and Miller [24] and Raynor [25] and thermodynamic properties such as partial enthalpy of mixing and activities in Mg–Ge liquid by Rao and Belton [28] and Eldridge et al. [29] and integral thermodynamic properties by Eldridge et al. [29] are used for this optimization. A four terms Redlich–Kister polynomial equation for the liquid phase is obtained from the optimization. The reference states for the Mg_2Ge compound are the Mg-hcp and Ge-diamond cubic and lattice stability values are not added for pure elements. The optimized model parameters for the liquid Mg–Ge phase and Mg_2Ge compound are given in Table 1. The calculated invariant points, along with the relevant literature values, are summarized in Table 2.

The heat and entropy of formation values of Mg_2Ge compound from the literature are given in Table 3. The values

Table 3
Thermodynamic properties of Mg_2Ge from the literature

Method	T (K)	$-\Delta H_f$ (J/(mol atom))	$-\Delta S_f$ (J/(mol atom K))	$-\Delta G_f$ (J/(mol atom))	Reference
emf	298	34750 ± 419			[28]
Solution calorimetry	273	38435 ± 83.7			[30]
Assessed	298		3.35 ± 4.19	37263 ± 1256	[30]
Solution calorimetry	273	38409 ± 83.7			[31]
Assessed	298		3.35 ± 4.18	37238 ± 1255	[31]
Thermodynamic modeling	298	39372.8	7.98	41750	This work

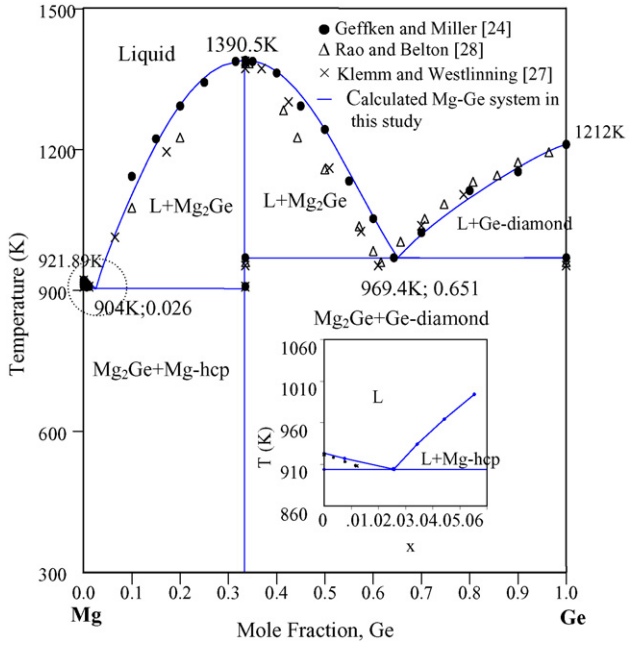

Fig. 6. Calculated Mg–Ge phase diagram with experimental points. The inset is a magnification of the Mg-rich side.

obtained in this work by thermodynamic modeling agree well with the values from the literature.

Fig. 6 shows the calculated Mg–Ge phase diagram with experimental data from the literature.

Figs. 7–9 show the calculated integral enthalpy, entropy and Gibbs free energy of mixing. They are compared with the experimental data of Eldridge et al. [29] and showed very good agreement.

The activities of Mg and Ge and partial molar enthalpy of Mg, in Mg–Ge liquid, are presented in Figs. 10 and 11, and they are compared with the experimental data from the literature and show good agreement.

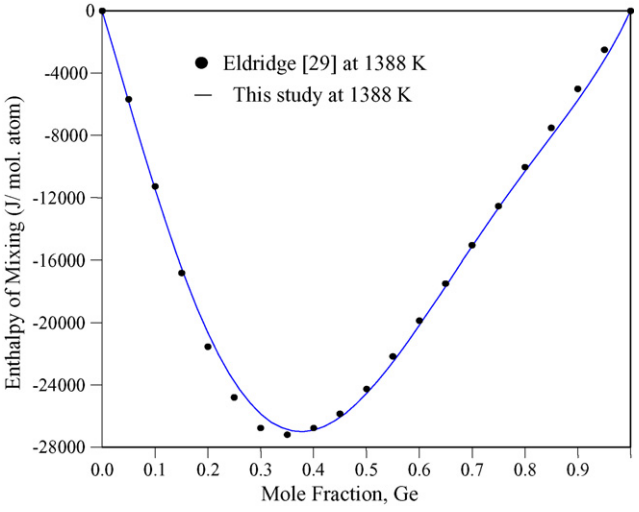

Fig. 7. Enthalpy of mixing of Mg–Ge liquid.

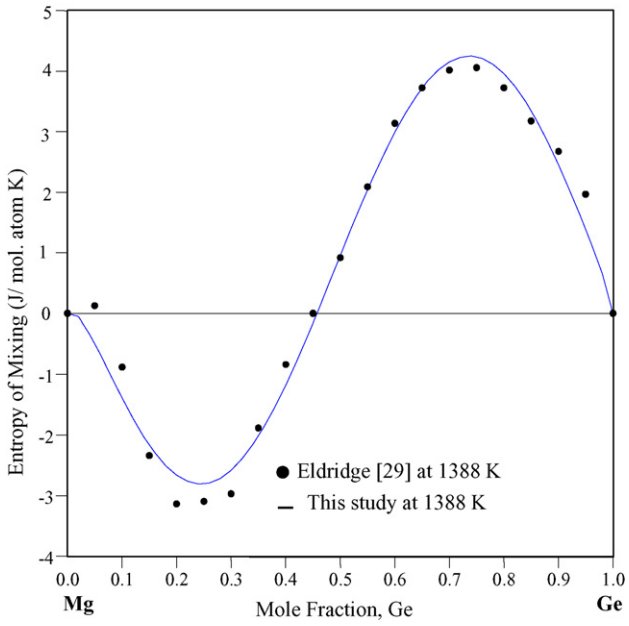

Fig. 8. Entropy of mixing of Mg–Ge liquid.

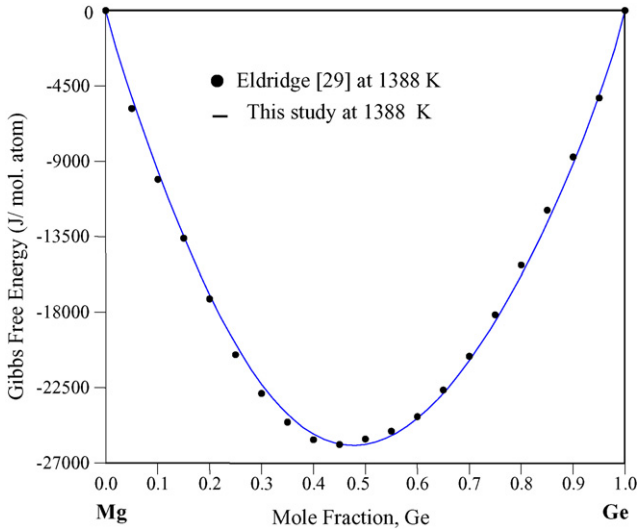

Fig. 9. Gibbs free energy of Mg–Ge liquid.

4. The Al–Mg system

Ansara et al. [4] generated the COST 507 database for light metal alloys. The optimized phase diagram and model parameters for the Al–Mg system were taken from the COST 507 database and reported in Table 4. For constructing the database for Mg–Al system, Ansara et al. [4] considered the experimental results of Liang et al. [32] as their work is the most recent and reliable one for this system. Redlich–Kister polynomial model is used for liquid phase and no lattice stability values were added for the pure elements, which made this Mg–Al database compatible with the other two binary systems: Al–Ge and Mg–Ge. Compatibility with existing models is crucial, if the resulting thermodynamic description is to be added to an existing database [8].

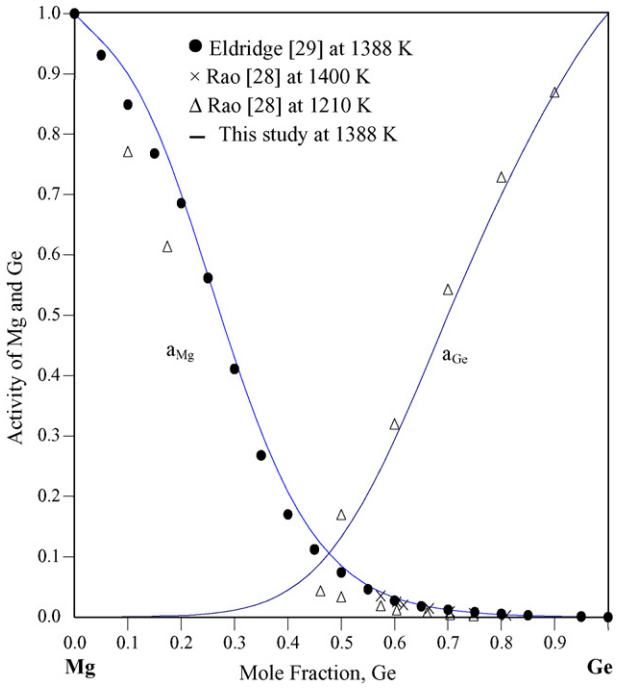

Fig. 10. Activity of Mg and Ge in Mg–Ge liquid.

Mg–Al system has: (1) liquid phase; (2) two terminal solid solutions Mg-hcp and Al-fcc; (3) two intermetallic compounds $Al_{30}Mg_{23}$ and $Al_{140}Mg_{89}$; (4) a non-stoichiometric compound $Mg_{17}Al_{12}$ (γ). The line compound $Al_{30}Mg_{23}$ (ε) is stable in the temperature range of 519.50–694.25 K. The congruent melting of $Al_{140}Mg_{89}$ (β) compound occurs at 723.89 K at the composition of 61.1 at.% Al and γ phase occurs at 738.49 K at the composition of 48.18 at.% Al. There are three eutectic reactions in this system: on the Al-rich side, L → β + Al-fcc, on the Mg-rich side, L → Mg-hcp + γ, and between γ and β, L → β + γ.

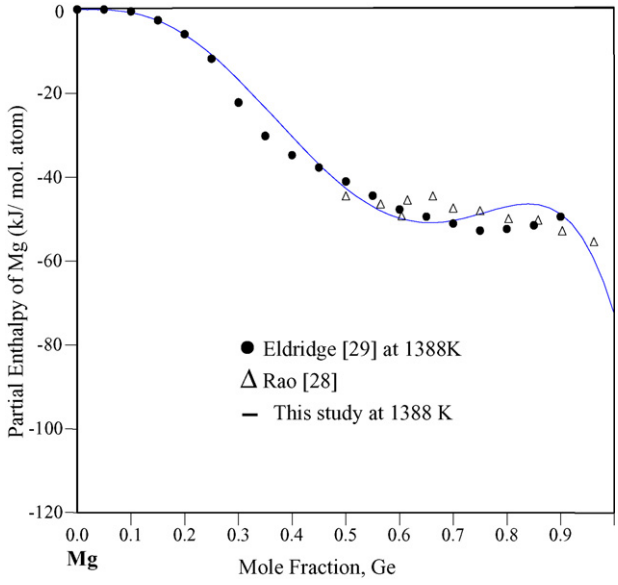

Fig. 11. Partial molar enthalpy of Mg in Mg–Ge liquid.

Table 4
Optimized model parameters for the Al–Mg system from COST 507 [4]

Phase	Parameter	*a*	*b*
Liquid	L_0	−12000	8.566
	L_1	1894	−3
	L_2	2000	0
$Al_{30}Mg_{23}$	ΔG_f	−986	−3.3125
$Al_{140}Mg_{89}$	ΔG_f	−1075	−2.935
$Al_{12}Mg_{17}$	*G*(Mg:Al:Al)	3375	−3.50
	G(Mg:Al:Mg)	7978	−4.60
	G(Mg:Mg:Al)	−1820	−1.92
	G(Mg:Mg:Mg)	4602.4	−2.80
	L(Mg;Al:Al, Mg)	113100	−14.50
	L(Mg:Mg:Al, Mg)	113100	−14.50

5. The Mg–Al–Ge ternary system

From the literature survey, it is found that only Badaeva and Kuznetsova [33] have done experimental study on the Al–Mg–Ge ternary system. They reported microstructures of different ternary alloys, some vertical sections of the ternary phase diagram and the Al-rich corner of the ternary diagram.

The Mg–Al–Ge ternary system is obtained by combining the thermodynamic description of the three binary systems: Al–Mg, Mg–Ge and Al–Ge with one additional ternary interaction parameter for the liquid phase. The optimized model parameters pertaining to the three binary and ternary systems and SGTE data [6] for pure elements are used to generate the ternary phase diagram. Ternary systems are presented by superimposing a series of liquidus lines from isothermal sections on the Gibbs triangle. The calculated Mg–Al–Ge ternary phase diagrams are shown in Figs. 12 and 13. The heavier lines represent the univariant valley. The arrows represent the direction of decreasing temperature along these lines. The temperature and composition of calculated ternary invariant points are listed in Table 5.

Four ternary eutectic and three saddle points are found from the calculated liquidus surface. One ternary eutectic point is close to the Al–Ge binary eutectic point and the other three ternary eutectic points are very close to the three binary eutectic points of the Al–Mg system. The binary eutectic points (e_1, e_2, e_3, e_4, e_5 and e_6), the ternary eutectic (E_1, E_2, E_3 and E_4) and the saddle points (Max_1, Max_2 and Max_3) are marked on the ternary phase diagram presented in Figs. 12 and 13. From the ternary phase diagram, it is clear that the Mg_2Ge compound dominates the ternary system. In order to graphically represent the three ternary eutectic and the two saddle points between β-Mg_2Ge and γ-Mg_2Ge on Mg–Al axis, close up views of the liquidus projection near the corresponding regions are shown in Fig. 12. In Mg–Al–Ge system, one ternary interaction parameter for the liquid phase

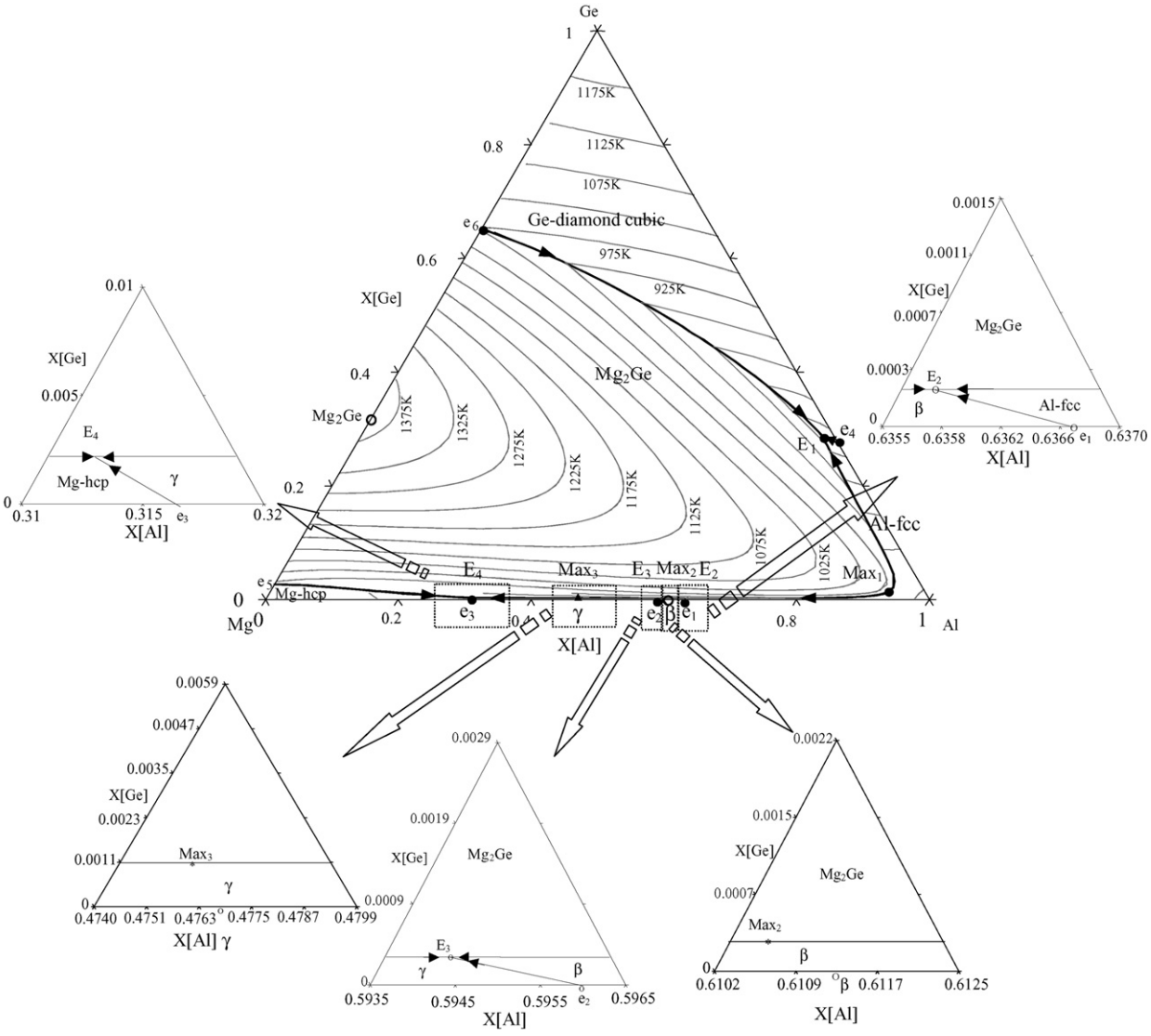

Fig. 12. Mg–Al–Ge calculated phase diagram in atomic fraction with enlarged part of liquidus projection near the Mg–Al axis.

has been introduced to have higher precision and better agreement with the experimental results. The value of the interaction parameter is shown in Table 1. Several vertical sections of the ternary system at different compositions are compared with the experimental data reported by Badaeva and Kuznetsova [33]. In Fig. 14(a–g), seven vertical sections are drawn. The calculated sections show very good agreement with the experimental results in most of the figures. Among them, the liquidus lines of vertical sections (a–e) show excellent agreement and vertical sections (f and g) show reasonable agreement.

Two quasi-binary phase diagrams have been calculated and shown in Fig. 15(a and b). The quasi-binary section between Al–Mg_2Ge in Fig. 15(a) shows very good agreement and Mg_2Ge–Al_3Mg_2 section in Fig. 15(b) shows reasonable agreement. For Figs. 14(f–g) and 15(b), it was possible to match the experimental results with the calculated diagram by changing the ternary interaction parameter but the consistency in the other figures was lost.

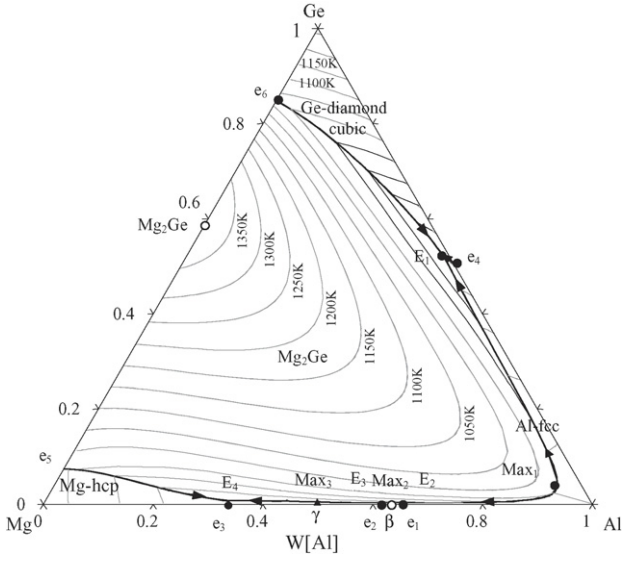

Fig. 13. Mg–Al–Ge calculated phase diagram in weight fraction.

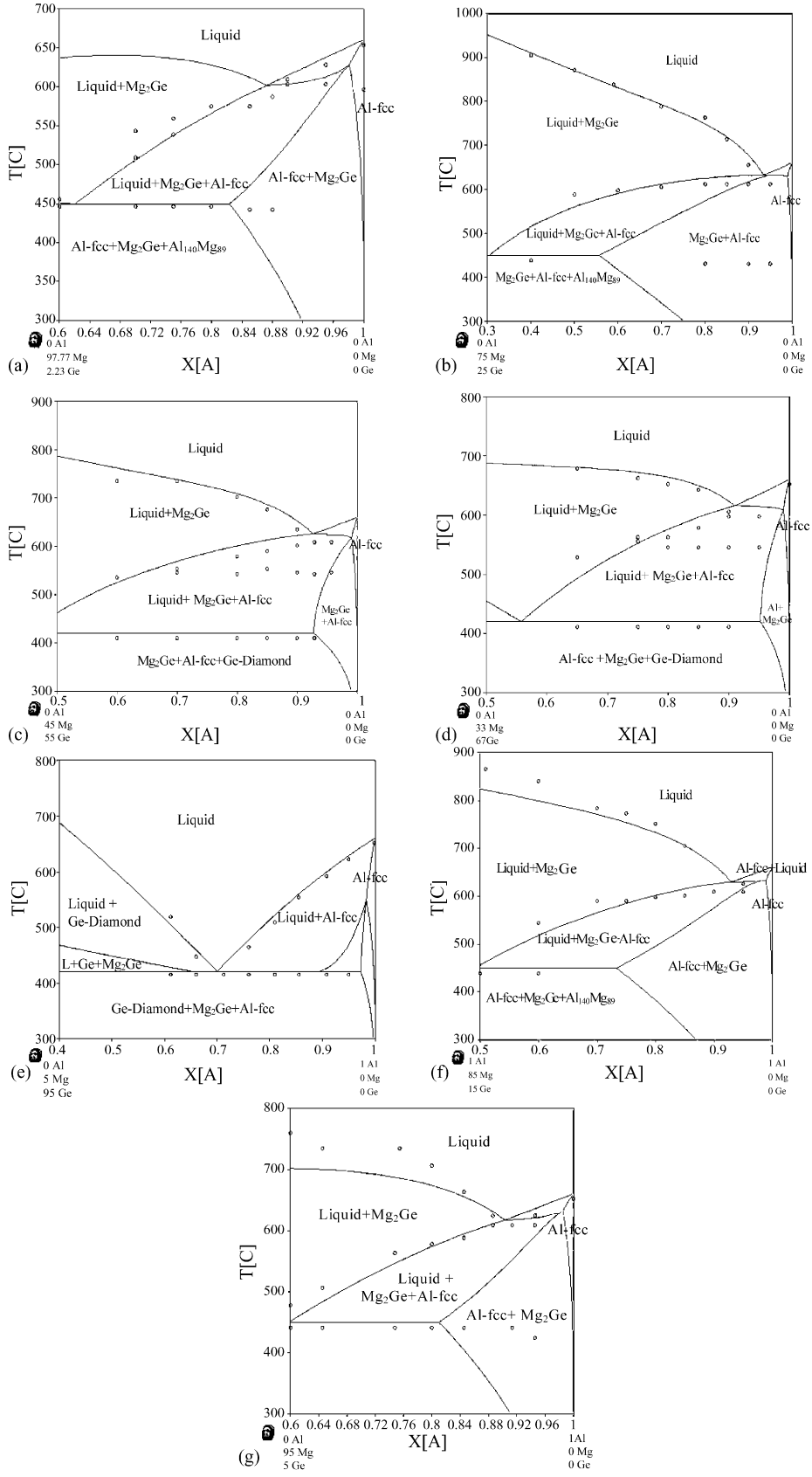

Fig. 14. Several vertical sections in the Mg–Al–Ge system in comparison with experimental data where (o) experimental data [33] and (—) calculated in this study. Section between: (a) Mg 97.77 at.% and Ge 2.23 at.% and Al-corner; (b) Mg 75 at.% and Ge 25 at.% and Al-corner; (c) Mg 45 at.% and Ge 55 at.% and Al-corner; (d) Mg 33 at.% and Ge 67 at.% and Al-corner; (e) Mg 5 at.% and Ge 95 at.% and Al-corner; (f) Mg 85 at.% and Ge 15 at.% and Al-corner; (g) Mg 95 at.% and Ge 5 at.% and Al-corner.

Table 5
Calculated invariant points for the Mg–Al–Ge ternary system

Reaction	T (K)	Composition (mole fraction)			Reaction type
		X_{Al}	X_{Mg}	X_{Ge}	
$L \rightarrow Mg_2Ge + Al\text{-fcc} + Ge\text{-diamond}$	692.554	0.6944	0.0182	0.2873	Ternary eutectic (E_1)
$L \rightarrow Mg_2Ge + Mg_{17}Al_{12} + Mg\text{-hcp}$	702.405	0.3119	0.6859	0.0021	Ternary eutectic (E_2)
$L \rightarrow Mg_2Ge + Al_{140}Mg_{89} + Al\text{-fcc}$	722.652	0.6357	0.3640	0.0002	Ternary eutectic (E_3)
$L \rightarrow Mg_2Ge + Mg_{17}Al_{12} + Al_{140}Mg_{89}$	723.266	0.5942	0.4053	0.0003	Ternary eutectic (E_4)
$L \rightarrow Mg_2Ge + Al\text{-fcc}$	905.175	0.9354	0.0449	0.0196	Saddle point (Max_1)
$L \rightarrow Al_{140}Mg_{89} + Mg_2Ge$	723.735	0.6105	0.3891	0.0003	Saddle point (Max_2)
$L \rightarrow Mg_{17}Al_{12} + Mg_2Ge$	738.048	0.4756	0.5231	0.0012	Saddle point (Max_3)

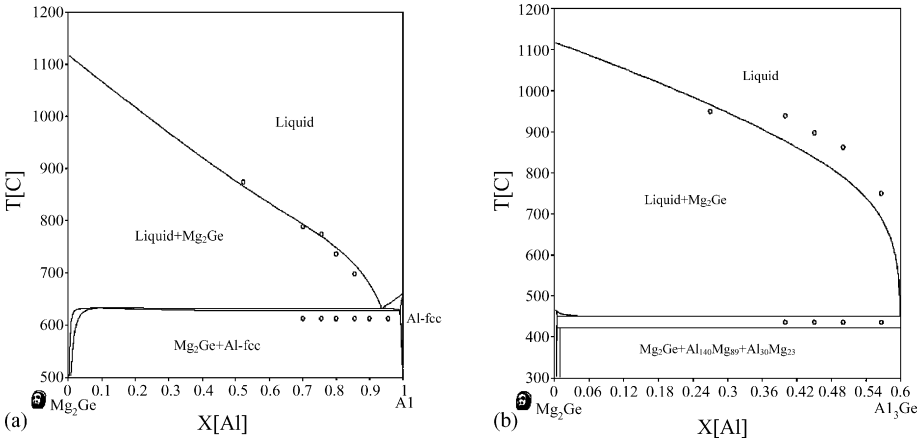

Fig. 15. Quasi-binary sections between (a) Mg_2Ge–Al and (b) Mg_2Ge–Al_3Mg_2.

6. Summary

Thermodynamic description for the Mg–Al–Ge system has been obtained. Al–Ge and Mg–Ge systems are thermodynamically optimized with the least number of coefficients. One ternary interaction coefficient has been introduced. The contribution of this parameter is necessary to improve the consistency with the experimental data from the literature. Using the optimized parameters, the binary phase diagrams, thermodynamic properties and ternary vertical sections are reproduced and are found to be in good agreement with the reported experimental results. This system has been thermodynamically modeled for the first time in this work and can be used to calculate higher order systems. The model can be used to predict thermodynamic properties, which might not be available in the literature.

Acknowledgments

This work was made possible by NSERC (Canada) and NATEQ (Quebec) grants.

References

[1] Z.K. Liu, CALPHAD and Alloy Thermodynamics, TMS (The Minerals, Metals and Materials Society) Annual Meeting, Seattle, WA, USA, February 17–21, 2002, pp. 205–214.
[2] K. Matsuda, T. Munekata, Y. Ishida, T. Sato, S. Ikeno, 8th Asia–Pacific Conference on Electron Microscopy, Kanazawa, Japan, June 7–11, 2004, pp. 801–802.
[3] T. Hasegawa, T. Yasuno, T. Nagai, T. Takahashi, Acta Metall. 46 (17) (1998) 6001–6007.
[4] I. Ansara, A.T. Dinsdale, M.H. Rand, European Commission EUR 18499, 1998.
[5] N. Saunders, A.P. Miodownik, Calculation of Phase Diagrams (CALPHAD): A Comprehensive Guide, Pergamon/Elsevier, Oxford, UK, 1998.
[6] A.T. Dinsdale, Calphad 15 (4) (1991) 317–425.
[7] H.L. Lukas, E. Henig, Th.B. Zimmermann, Calphad 1 (3) (1977) 225–236.
[8] P. Chartrand, A.D. Pelton, J. Phase Equilib. 15 (6) (1994) 591–605.
[9] N. Ansara, Int. Metals Rev. 24 (1) (1979) 20–53.
[10] WinPhaD—Phase Diagram Calculation Engine for Multicomponent Systems, Computherm LLC, Madison, WI, USA, 2000.
[11] S. Srikanth, D. Sanyal, P. Ramachandrarao, Calphad 20 (3) (1996) 321–332.
[12] W. Kroll, Metall und Erz 23 (1926) 682–684.
[13] H. Stohr, W. Klemm, Z. Anorg. Allg. Chem. 241 (1939) 305–313.
[14] T.C. Wilder, Trans. Metall. AIME 236 (1) (1966) 88–94.
[15] H. Eslami, J. Franceschi, M. Gambino, J.P. Bros, Z. Naturforsch. 34 (7) (1979) 810–817.
[16] J.M. Caywood, Metall. Trans. 4 (3) (1973) 735–743.
[17] V.M. Glazov, T.-J. Chien, C.-Y. Liu, Russ. J. Inorg. Chem. 7 (1962) 293–296.
[18] Y. Minamino, T. Yamane, H. Araki, T. Adachi, Y. Kang, Y. Miyamoto, T. Okamoto, J. Mater. Sci. 26 (20) (1991) 5623–5630.
[19] G.I. Batalin, E.A. Belaborodova, Russ. J. Phys. Chem. 42 (3) (1968) 781–784.
[20] V.B. Predel, D.W. Stein, Z. Metallkd. 62 (6) (1971) 499–504.
[21] H. Eslami, Y.M. Muggianu, M. Gambino, J.P. Bros, J. Less-Common Met. 64 (1) (1979) 31–44.
[22] A.J. McAlister, J.L. Murray, Bull. Alloy Phase Diagrams 5 (4) (1984) 341–347.
[23] L. Kaufman, Calphad 3 (1) (1979) 45–76.
[24] R. Geffken, E. Miller, Trans. Metall. AIME 242 (1968) 2323–2328.
[25] G.V. Raynor, J. Inst. Met. 66 (12) (1940) 403–426.

[26] A.A. Nayeb-Hashemi, J.B. Clark, R.W. Olesinski, G.J. Abbaschian, Bull. Alloy Phase Diagrams 5 (4) (1984) 359–365.
[27] W. Klemm, H. Westlinning, Z. Anorg. Chem. 245 (1941) 365–380.
[28] Y.K. Rao, G.R. Belton, Metall. Trans. 2 (1971) 2215–2219.
[29] J.M. Eldridge, E. Miller, K.L. Komarek, Trans. Metall. AIME 236 (1966) 1094–1097.
[30] P. Beardmore, B.W. Howlett, B.D. Lichter, M.B. Bever, Trans. Metall. AIME 236 (1966) 102–108.
[31] M.B. Bever, B.W. Howlett, S. Misra, P.M. Robinson, P. Beardmore, Project 5620, Task 562001, Final Report, Massachusetts Institute of Technology, Cambridge, MA, USA, 1964.
[32] P. Liang, H.L. Su, P. Donnadieu, M. Harmelin, A. Quivy, Philos. Mag. A 78 (4) (1998) 893–905.
[33] T.A. Badaeva, R.I. Kuznetsova, Trudy Inst. Met. Im. A.A. Baikova 3 (1958) 217–230.